EUROPEAN JOURNAL OF COMPUTATIONAL MECHANICS
2018, VOL. 27, NO. 2, 123–142
https://doi.org/10.1080/17797179.2018.1484032

Taylor & Francis
Taylor & Francis Group

The influence of higher in- and out-of-plane natural modes on dynamic pull-in instability of electrically actuated micro-plates

Amir R Askari

Department of Mechanical Engineering, Hakim Sabzevari University, Sabzevar, Iran

ABSTRACT

Generating reduced-order models (ROMs) is one of the most efficient procedures for predicting pull-in instability threshold in electrically actuated rectangular micro-plates. To date, there exist some different approaches for this procedure in the literature with different numbers of employed natural modes which yield different results. The main objective of the present paper is to answer the basilar question of how many natural modes for discretising the in- and out-of-plane displacements should be included to ensure an efficient ROM. To this end, a full geometric non-linear Kirchhoff's plate model with fully clamped boundary conditions, which accounts for both in-plane and transverse displacements is considered. A multi-mode ROM is also developed and both static and dynamic instability thresholds of the system are extracted. Convergence studies on both static and dynamic findings are also performed to illustrate the importance of each in- or out-of-plane mode on the accuracy of the results. Utilising the present convergence studies, the minimum number of in- and out-of-plane modes, which should be employed to achieve precise predictions, is determined. At the rest of the paper, effect of micro-plate inertia on reducing the instability threshold of systems with different initial gaps and aspects ratios is also studied in details.

ARTICLE HISTORY
Received 27 December 2017
Accepted 2 May 2018

KEYWORDS
Electrically actuated rectangular micro-plates; pull-in instability; reduced-order model; number of employed natural modes

1. Introduction

Technology of micro-electro-mechanical systems (MEMS) has experienced many improvements in recent years. Because of their small size, low power consumption, reliability and their capability of batch fabrications, they have found lots of potential applications in engineering. The building blocks of these systems are some sort of electrically actuated mechanical structures such as bars, beams or plates (Senturia, 2001). In general, an electrically actuated micro-plate is a conductive and elastic thin plate suspended over a stationary rigid electrode and deflects toward its substrate by applying the external voltage (Batra, Porfiri, & Spinello, 2007). By

CONTACT Amir R Askari amaskari@gmail.com

increasing the values of the applied voltage, the Coulomb attraction between the movable electrode and its rigid substrate is also increased which results in the increase of the micro-plate deflection. The applied voltage has an upper limit in which the elastic restoring force of the movable electrode cannot resist against the Coulomb attraction and this electrode suddenly collapses toward the substrate underneath it (Batra et al., 2007). This unstable behavior is called pull-in instability and the upper limit of the applied voltage is also named as the pull-in voltage (Batra et al., 2007).

Due to the coupling between electrical and structural physics as well as the strong non-linearities arising in the field of electrically actuated micro-structures, modelling of MEMS is so challenging (Younis, 2011). To date, variety of numerical procedures such as the finite element (FE) (Tajalli, Moghimi Zand, & Ahmadian, 2009) and differential quadrature (Ansari, Gholami, Mohammadi, & Faghih Shojaei, 2012; Wang, Zhou, Zhao, & Chen, 2011) methods as well as generating reduced-order (RO) models (Batra, Porfiri, & Spinello, 2008a, 2008b; Zhao, Abdel-Rahman, & Nayfeh, 2004) have been employed to uncover the behaviors of electrically actuated micro-plates. Amongst all of these procedures, generating reduced-order models (ROMs) enjoys several attractive features such as the robustness over the whole operation range of the device, low run-time and providing the ability of presenting semi-analytical solutions (Zhao et al., 2004).

In view of the available ROMs for plate-type MEMS in the literature, it can be observed that there exist different types of this method with different numbers of basis functions in the discretisation procedure. For example, Zhao et al. (2004) studied statics and free vibrations of electrically actuated rectangular micro-plates in which the effects of non-linear von Kármán strains had been taken into account. They utilised the Galerkin-weighted residual method (GWRM) with the linear mode-shapes of the system as the basis functions. It is worth mentioning that since the linear out-of-plane mode-shapes of fully clamped rectangular micro-plates cannot be obtained analytically, they employed the hierarchical finite element method (HFEM) to determine these basis functions. In addition, they approximated the in-plane displacements in terms of the transverse generalised coordinates through the HFEM and retained eight out-of-plane eigen modes in their RO procedure to achieve precise predictions. Batra et al. (2008b) analyzed the influence of Casimir attraction on static and free vibration responses of electrostatically actuated fully clamped rectangular and circular micro-plates. They also presented another work which investigated the effect of thermal stresses on rectangular micro-plates subjected to the van der Waals force (Batra et al., 2008a). In these two studies, they accounted for the effect of von Kármán non-linear strains and employed the GWRM with the in-plane and transverse basis functions, respectively, approximated by sinusoidal functions and the product

of doubly clamped beam mode-shapes for micro-plates with the rectangular shape. It is worth noting that their model, which include one and nine basis functions, respectively, for the transverse and each in-plane displacement, could predict the static pull-in voltage and the fundamental frequency of the system in good agreement with those reported by Zhao et al. (2004). Chao, Chiu, and Tsai (2006) studied static pull-in instability in geometric linear micro-plates. They employed a single-term GWRM, expanded the electrostatic forcing term up to the fifth order and extracted an explicit expression for the static pull-in voltage of the system. Talebian, Rezazadeh, Fathalilou, and Toosi (2010) investigated the influence of temperature on static pull-in and free vibrations of geometric non-linear micro-plates. Nabian, Rezazadeh, Almassi, and Borgheei (2013) also presented a similar work for systems made of functionally graded materials. It is to be mentioned here that the authors of the latest two studies (Nabian et al., 2013; Talebian et al., 2010) approximated the transverse deflection by employing only one eigen mode and set the values of the in-plane displacements to zero. Mohammadi and Ali (2015) investigated the effect of thermoelastic damping on the natural frequencies of electrically pre-deformed micro-plates. They accounted for the effect of geometric non-linearity together with the in-plane displacements and solved the set of the governing equations through the GWRM. They approximated each component of the in-plane displacements with only one basis function. Saghir and Younis (2016) studied the static pull-in instability as well as the primary and secondary resonances of the fundamental mode of fully clamped rectangular micro-plates under the application of AC voltages superimposed to statically applied DC ones. They employed COMSOL Multiphysics commercial software to extract both in- and out-of-plane basis functions, respectively, by performing stationary and free vibration studies in this software. Using these basis functions, they solved the set of governing equations of motion through the GWRM, in which the in- and out-of-plane displacements have been discretised by considering one and five basis functions, respectively. They compared and validated their model's predictions by those obtained using COMSOL Multiphysics. Furthermore, they illustrated that their procedure does not suffer from long run-time in comparison to the three-dimensional (3-D) FE simulations.

According to the aforementioned literature, it is observed that there exist some differences between the number of employed in- and out-of-plane basis functions in the discretising procedure: some researchers employed only the first natural mode for discretising the transverse deflection (Batra et al., 2008a, 2008b; Chao et al., 2006; Mohammadi & Ali, 2015; Nabian et al., 2013; Talebian et al., 2010), while some others believed that higher out-of-plane natural modes should be included into the RO procedure to ensure the accuracy of the results (Saghir & Younis, 2016; Zhao et al., 2004); also the number of employed in-plane basis functions in some published works (Batra et al., 2008a, 2008b;

Mohammadi & Ali, 2015; Nabian et al., 2013; Saghir & Younis, 2016; Talebian et al., 2010) differs from each other. Therefore, the main object of the present study is to provide a multi-mode ROM for full geometric non-linear plate-type MEMS with fully clamped boundary conditions and investigate the importance of each eigen mode on the accuracy of the results. In addition, by removing the non-significant natural modes from the model, an optimised ROM with the minimum number of essential approximating functions for both in- and out-of-plane displacements is introduced.

The rest of the paper is organised as follows. In Section 2, the mathematical model of the system is represented briefly. In Section 3, the details of developing our efficient ROM are explained. In Section 4, the static results of the present study are compared and validated by those available in the literature. However, due to the lack of multi-mode dynamic results in the previous studies, the present dynamic findings are compared with those obtained by 3-D FE simulations carried out in COMSOL Multiphysics commercial package COMSOL, 2016. The rest of this section is also devoted to a detailed parametric study which emphasises on the significant effect of the micro-plate inertia on the instability threshold of systems with different initial gaps and aspect ratios. The main conclusions of the present work are also summarised in Section 5.

2. Theoretical formulation

Figure 1 shows an electrically actuated rectangular micro-plate whose length, width, thickness and density are denoted by b, a, h and ρ, respectively. The initial gap between the non-actuated micro-plate and the substrate is assumed to be d. Utilising the non-linear Kirchhoff plate model in which the strain-displacement relations have been approximated by the von Kármán theory, the governing equations of motion take the form (Zhao et al., 2004):

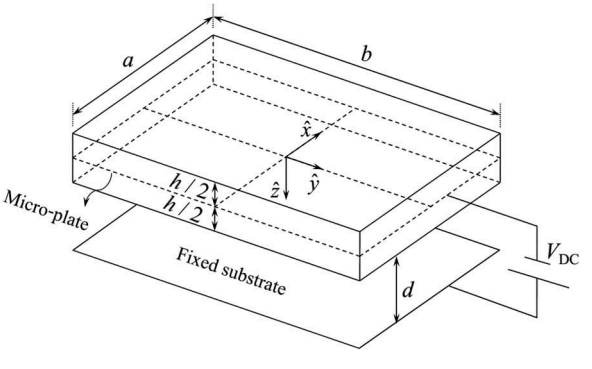

Figure 1. Schematic of an electrically actuated rectangular micro-plate.

$$\hat{u}_{,\hat{x}\hat{x}} + \hat{w}_{,\hat{x}}\hat{w}_{,\hat{x}\hat{x}} + \frac{1-\nu}{2}\left(\hat{u}_{,\hat{y}\hat{y}} + \hat{w}_{,\hat{x}}\hat{w}_{,\hat{y}\hat{y}}\right) + \frac{1+\nu}{2}\left(\hat{v}_{,\hat{x}\hat{y}} + \hat{w}_{,\hat{y}}\hat{w}_{,\hat{x}\hat{y}}\right) = 0 \quad (1a)$$

$$\hat{v}_{,\hat{y}\hat{y}} + \hat{w}_{,\hat{y}}\hat{w}_{,\hat{y}\hat{y}} + \frac{1-\nu}{2}\left(\hat{v}_{,\hat{x}\hat{x}} + \hat{w}_{,\hat{y}}\hat{w}_{,\hat{x}\hat{x}}\right) + \frac{1+\nu}{2}\left(\hat{u}_{,\hat{x}\hat{y}} + \hat{w}_{,\hat{x}}\hat{w}_{,\hat{x}\hat{y}}\right) = 0 \quad (1b)$$

$$\begin{aligned}\rho h\hat{w}_{,\hat{t}\hat{t}} + \frac{Eh^3}{12(1-\nu^2)}\nabla^4\hat{w} = \frac{Eh}{1-\nu^2}\Bigg[\hat{w}_{,\hat{x}\hat{x}}\left(\hat{u}_{,\hat{x}} + \frac{1}{2}\left(\hat{w}_{,\hat{x}}\right)^2 + \nu\hat{v}_{,\hat{y}} + \frac{\nu}{2}\left(\hat{w}_{,\hat{y}}\right)^2\right)\\ + (1-\nu)\hat{w}_{,\hat{x}\hat{y}}\left(\hat{u}_{,\hat{y}} + \hat{v}_{,\hat{x}} + \hat{w}_{,\hat{x}}\hat{w}_{,\hat{y}}\right) + \hat{w}_{,\hat{y}\hat{y}}\left(\hat{v}_{,\hat{y}} + \frac{1}{2}\left(\hat{w}_{,\hat{y}}\right)^2 + \nu\hat{u}_{,\hat{x}} + \frac{\nu}{2}\left(\hat{w}_{,\hat{x}}\right)^2\right)\Bigg]\\ + \frac{\varepsilon\, V_{\mathrm{DC}}^2}{2(d-\hat{w})^2}\end{aligned} \quad (1c)$$

where $\hat{u}$, $\hat{v}$ and $\hat{w}$ are the displacements along the $\hat{x}$, $\hat{y}$ and $\hat{z}$ directions, respectively; $\hat{t}$ is the time, E is the Young modulus, ν is the Poisson ratio, ε is the dielectric constant of the media and V_{DC} is the external applied voltage. Also the comma sign followed by an independent variable refers to the partial derivative with respect to that variable and the ∇^4 operator for a two-dimensional Cartesian space is expressed as:

$$\nabla^4 = \left(\frac{\partial^4}{\partial\hat{x}^4} + 2\frac{\partial^4}{\partial\hat{x}^2\partial\hat{y}^2} + \frac{\partial^4}{\partial\hat{y}^4}\right) \quad (2)$$

Introducing the dimensionless variables $u = \frac{a\hat{u}}{d^2}$, $v = \frac{b\hat{v}}{d^2}$, $w = \frac{\hat{w}}{d}$, $x = \frac{\hat{x}}{a}$, $y = \frac{\hat{y}}{b}$ and $t = \hat{t}/T$, the non-dimensionalised form of the governing equations of motion in (1) are expressed as:

$$\begin{aligned}u_{,xx} + w_{,x}w_{,xx} + \frac{\alpha_1^2(1-\nu)}{2}\left(u_{,yy} + w_{,x}w_{,yy}\right)\\ + \frac{\alpha_1^2(1+\nu)}{2}\left(v_{,xy} + w_y w_{,xy}\right) = 0\end{aligned} \quad (3a)$$

$$\begin{aligned}\alpha_1^4\left(v_{,yy} + w_{,y}w_{,yy}\right) + \frac{\alpha_1^2(1-\nu)}{2}\left(v_{,xx} + w_{,y}w_{,xx}\right)\\ + \frac{\alpha_1^2(1+\nu)}{2}\left(u_{,xy} + w_x w_{,xy}\right) = 0\end{aligned} \quad (3b)$$

$$\left(\frac{1}{12}\right)\left(w_{,xxxx}+2\alpha_1^2 w_{,xxyy}+\alpha_1^4 w_{,yyyy}\right)+w_{,tt}=\frac{\alpha_2}{(1-w)^2}$$
$$+\alpha_3^2\left\{w_{,xx}\left[u_{,x}+\frac{1}{2}w_{,x}^2+\nu\alpha_1^2\ \times\left(v_{,y}+\frac{1}{2}w_{,y}^2\right)\right]\right.$$
$$+w_{,xy}\left[(1-\nu)\alpha_1^2\left(u_{,y}+v_{,x}+w_{,x}w_{,y}\right)\right]$$
$$\left.+w_{,yy}\left[\alpha_1^4\left(v_{,y}+\frac{1}{2}w_{,y}^2\right)+\nu\ \times\left(u_{,x}+\frac{1}{2}w_{,x}^2\right)\right]\right\} \tag{3c}$$

in which the normalized parameters of the problem are as follows:

$$\alpha_1=\frac{a}{b},\ \alpha_2=\frac{\varepsilon a^4(1-\nu^2)V_{\mathrm{DC}}^2}{2Eh^3d^3},\ \alpha_3=\frac{d}{h} \tag{4}$$

Also, the timescale T, which is determined such that the coefficient of $w_{,tt}$ becomes unity, is defined as:

$$T=\sqrt{\frac{\rho a^4(1-\nu^2)}{Eh^2}} \tag{5}$$

It is noteworthy to mention that, hereinafter, the normalized parameters α_1, α_2 and α_3 are named as the micro-plate aspect ratio, the electrostatic and gap parameters, respectively. Also the non-dimensional form of the boundary conditions for present micro-plate with fully clamped and immovable edges can be expressed as:

$$u=v=w=w_{,x}=w_{,y}=0\ \text{at}\ x=\pm\frac{1}{2} \tag{6a}$$

$$u=v=w=w_{,x}=w_{,y}=0\ \text{at}\ y=\pm\frac{1}{2} \tag{6b}$$

3. The reduced-order model

Due to the high-non-linearity involved in the system of PDEs in (3), analytical solution for this set of equations is not proposed yet. Therefore, an approximate solution based on the GWRM will be developed here. To this end, the dimensionless displacements u, v and w are discretised as follow:

$$u(x,y,t)=\sum_{i=1}^{n}\sum_{j=1}^{n}u_{ij}(t)\varphi_u^{ij}(x,y) \tag{7a}$$

$$v(x,y,t) = \sum_{i=1}^{n}\sum_{j=1}^{n} v_{ij}(t)\varphi_v^{ij}(x,y) \tag{7b}$$

$$w(x,y,t) = \sum_{i=1}^{m}\sum_{j=1}^{m} w_{ij}(t)\varphi_w^{ij}(x,y) \tag{7c}$$

where u_{ij}, v_{ij} and w_{ij} are the generalised coordinates which should be determined during the GWRM. Also $\varphi_u^{ij}(x,y)$, $\varphi_v^{ij}(x,y)$ and $\varphi_w^{ij}(x,y)$ are the GWRM admissible basis functions which, respectively, approximate the displacements u, v and w and identically satisfy all associated boundary conditions presented in Eq. (6). Furthermore, n and m refer to the number of in- and out-of-plane approximating functions in each direction of x and y, respectively.

In the present work, the linear undamped mode-shapes of the system are selected as the GWRM admissible basis functions. It is to be mentioned here that although the in-plane mode-shapes for the present micro-plate with immovable edges can analytically be obtained as sinusoidal functions (Batra et al., 2008b), there exist no analytical solution for the transverse ones. Hence, in the present study, the out-of-plane mode-shapes of the structure is obtained semi-analytically through the extended Kantorovich method (for more details, see the work of Jones & Milne, 1976). It is noteworthy that, due to the symmetry of the present system, only the symmetric out-of-plane mode-shapes are retained in the RO procedure and the in-plane approximating functions have been chosen as (Amabili, 2004):

$$\varphi_u^{ij}(x,y) = \sin\left[2i\pi\left(x+\frac{1}{2}\right)\right]\sin\left[(2j-1)\pi\left(y+\frac{1}{2}\right)\right] \tag{8a}$$

$$\varphi_v^{ij}(x,y) = \sin\left[(2i-1)\pi\left(x+\frac{1}{2}\right)\right]\sin\left[2j\pi\left(y+\frac{1}{2}\right)\right] \tag{8b}$$

By substituting Eqs. (7) into Eqs. (3a) and (3b) and also, according to the GWRM, multiplication of both sides of each equation by its respective approximating function, the values of unknown in-plane displacements u and v can readily be obtained in terms of the transverse generalised coordinates. It is to be mentioned here that, for the purpose of simplicity, the displacements u, v and w are rewritten using single sub/superscript notation as follow:

$$u(x,y,t) = \sum_{p=1}^{n^2} u_p(t)\varphi_u^p(x,y) \tag{9a}$$

$$v(x,y,t) = \sum_{p=1}^{n^2} v_p(t)\varphi_v^p(x,y) \tag{9b}$$

$$w(x,y,t) = \sum_{p=1}^{m^2} w_p(t)\varphi_w^p(x,y) \tag{9c}$$

where in Eqs. (9a) and (9b), the sub/superscript p relates to the sub/superscripts i and j through $p = n(i-1)+j$, and in Eq. (9c) the sub/superscript p relates to the sub/superscripts i and j by $p = m(i-1)+j$. By applying the abovementioned GWRM on Eqs. (3a) and (3b), one would get:

$$u = \sum_{i=1}^{m^2}\sum_{j=1}^{m^2}\sum_{p=1}^{n^2} \varphi_u^p \Lambda_p^{ij} w_i w_j \tag{10a}$$

$$v = \sum_{i=1}^{m^2}\sum_{j=1}^{m^2}\sum_{p=1}^{n^2} \varphi_v^p \Gamma_p^{ij} w_i w_j \tag{10b}$$

in which:

$$\begin{Bmatrix} \Lambda_p^{ij} \\ \Gamma_p^{ij} \end{Bmatrix}_{2n\times 1} = -\begin{bmatrix} K_{pq}^1 & K_{pq}^2 \\ K_{pq}^3 & K_{pq}^4 \end{bmatrix}_{2n\times 2n}^{-1} \begin{Bmatrix} {}^1F_q^{ij} \\ {}^2F_q^{ij} \end{Bmatrix}_{2n\times 1} \tag{11}$$

where:

$$K_{pq}^1 = \iint_A \left[\varphi_{u,xx}^p + \frac{\alpha_1^2(1-\nu)}{2}\varphi_{u,yy}^p\right]\varphi_u^q dA \tag{12a}$$

$$K_{pq}^2 = \iint_A \left[\frac{\alpha_1^2(1+\nu)}{2}\varphi_{v,xy}^p\right]\varphi_u^q dA \tag{12b}$$

$$K_{pq}^3 = \iint_A \left[\frac{\alpha_1^2(1+\nu)}{2}\varphi_{u,xy}^p\right]\varphi_v^q dA \tag{12c}$$

$$K_{pq}^4 = \iint_A \left[\alpha_1^4\varphi_{v,yy}^p + \frac{\alpha_1^2(1-\nu)}{2}\varphi_{v,xx}^p\right]\varphi_v^q dA \tag{12d}$$

$$\begin{aligned} {}^1F_q^{ij} = \iint_A [&\varphi_{w,x}^i\varphi_{w,xx}^j + \frac{\alpha_1^2(1-\nu)}{2}\varphi_{w,x}^i\varphi_{w,yy}^j \\ &+ \frac{\alpha_1^2(1+\nu)}{2}\varphi_{w,y}^i\varphi_{w,xy}^j]\varphi_u^q dA \end{aligned} \tag{12e}$$

$$
\begin{aligned}
{}^{2}F_{q}^{ij} = \iint_{A} [&\alpha_1^4 \varphi_{w,y}^{i} \varphi_{w,yy}^{j} + \frac{\alpha_1^2(1-\nu)}{2} \varphi_{w,y}^{i} \varphi_{w,xx}^{j} \\
&+ \frac{\alpha_1^2(1+\nu)}{2} \varphi_{w,x}^{i} \varphi_{w,xy}^{j}] \varphi_{\nu}^{q} dA
\end{aligned}
\tag{12f}
$$

To complete the procedure and generate the ROM, it is sufficient to substitute Eqs. (9c), (10a) and (10b) into Eq. (3c). Multiplying both sides of Eq. (3c) by $\varphi_w^p(x,y)$ and integrating the outcome over the whole dimensionless region A. Doing so, the ROM associated with the PDEs of motion in (3), is obtained as:

$$
\begin{aligned}
&\sum_{m^2}^{s=1} \mathcal{M}_{rs} \ddot{w}_s + \sum_{m^2}^{s=1} \mathcal{K}_{rs} w_s - \alpha_3^2 \mathrm{H}_r \\
&- \alpha_2 \iint_{A} \varphi_w^r \left(1 - \sum_{m^2}^{s=1} \varphi_w^s w_s\right)^{-2} dA = 0
\end{aligned}
\tag{13}
$$

where:

$$
\mathcal{M}_{rs} = \iint_{A} \varphi_w^r \varphi_w^s dA \tag{14a}
$$

$$
\mathcal{K}_{rs} = \frac{1}{12} \iint_{A} (\varphi_{w,xxxx}^{s} + 2\alpha_1^2 \varphi_{w,xxyy}^{s} + \alpha_1^4 \varphi_{w,yyyy}^{s}) \varphi_w^r dA \tag{14b}
$$

$$
\begin{aligned}
\mathrm{H}_r = \sum_{i,j,k=1}^{m^2} \Bigg\{ &\left(\sum_{p=1}^{n^2} \Lambda_p^{ij} \iint_{A} \varphi_{w,xx}^{k} \varphi_{u,x}^{p} \varphi_w^r dA \right) + \frac{1}{2} \iint_{A} \varphi_{w,x}^{i} \varphi_{w,x}^{j} \varphi_{w,xx}^{k} \varphi_w^r dA \\
&+ \nu\alpha_1^2 \left[\left(\sum_{p=1}^{n^2} \Gamma_p^{ij} \iint_{A} \varphi_{w,xx}^{k} \varphi_{v,y}^{p} \varphi_w^r dA \right) + \frac{1}{2} \iint_{A} \varphi_{w,y}^{i} \varphi_{w,y}^{j} \varphi_{w,xx}^{k} \varphi_w^r dA \right] \\
&+ \alpha_1^4 \left[\left(\sum_{p=1}^{n^2} \Gamma_p^{ij} \iint_{A} \varphi_{w,yy}^{k} \varphi_{v,y}^{p} \varphi_w^r dA \right) + \frac{1}{2} \iint_{A} \varphi_{w,y}^{i} \varphi_{w,y}^{j} \varphi_{w,yy}^{k} \varphi_w^r dA \right] \\
&+ \nu \left[\left(\sum_{p=1}^{n^2} \Lambda_p^{ij} \iint_{A} \varphi_{w,yy}^{k} \varphi_{u,x}^{p} \varphi_w^r dA \right) + \frac{1}{2} \iint_{A} \varphi_{w,x}^{i} \varphi_{w,x}^{j} \varphi_{w,yy}^{k} \varphi_w^r dA \right] \\
&+ (1-\nu)\alpha_1^2 \left[\left(\sum_{p=1}^{n^2} \Lambda_p^{ij} \iint_{A} \varphi_{w,xy}^{k} \varphi_{u,y}^{p} \varphi_w^r dA \right) + \iint_{A} \varphi_{w,x}^{i} \varphi_{w,y}^{j} \varphi_{w,xy}^{k} \varphi_w^r dA \right. \\
&\left. + \left(\sum_{p=1}^{n^2} \Gamma_p^{ij} \iint_{A} \varphi_{w,xy}^{k} \varphi_{v,x}^{p} \varphi_w^r dA \right) \right] \Bigg\} w_i w_j w_k
\end{aligned}
\tag{14c}
$$

The dynamics of the system will be obtained through the solution of the reduced equations in (13). In the present paper, this set of equations will be solved using the fourth order Runge-Kutta method (Faires & Burden, 2002) with zero initial conditions. The static configuration of a statically excited system will also be obtained through the application of the Newton-Raphson procedure (Faires & Burden, 2002) on the ROM presented in Eq. (13) when the inertia terms are neglected (i.e. $\mathcal{M}_{rs} = 0$). It is worth noting that although the present ROM contains $2n^2 + m^2$ basis functions, it has m^2 degrees of freedom.

4. Results and discussions

4.1. *Model verification*

To find the number of modes which should be included into the present ROM, convergence studies on static and dynamic pull-in parameters are performed, respectively, in Tables 1 and 2 for a square micro-plate with normalized properties $\alpha_3 = 1$ and $\nu = 0.3$. According to the results of Tables 1 and 2, both static and dynamic pull-in parameters will completely be converged if the number of transverse and in-plane modes in each direction is set to $m = 1$ and $n = 3$, respectively. Therefore, in what follows, only the first transverse mode is employed and three in-plane basis functions at each direction in the ROM are retained to ensure the accuracy of the results. It is worth noting that by removing the unnecessary natural modes from the present ROM, it contains $2n^2 + 1$ basis functions and only one degree of freedom. Hence, the present ROM will be fast convergent and so rapid; because the response of the device can easily be obtained by solving only a single ODE in time. This important feature of the present ROM provides the ability of presenting analytical or semi-analytical solutions for complex problems arising in the field of plate-type MEMS which can be utilised in future studies.

Table 1. Convergence of the static pull-in parameter for a square micro-plate with normalized properties $\alpha_3 = 1$ and $\nu = 0.3$.

	$n = 0$	$n = 1$	$n = 2$	$n = 3$	$n = 4$
$m = 1$	15.05	15.16	16.05	16.06	16.06
$m = 2$	14.98	15.09	16.05	16.06	16.06
$m = 3$	14.98	15.09	16.05	16.06	16.06

Table 2. Convergence of the dynamic pull-in parameter for a square micro-plate with normalized properties $\alpha_3 = 1$ and $\nu = 0.3$.

	$n = 0$	$n = 1$	$n = 2$	$n = 3$	$n = 4$
$m = 1$	12.40	12.64	13.25	13.26	13.26
$m = 2$	12.34	12.58	13.25	13.26	13.26
$m = 3$	12.34	12.58	13.25	13.26	13.26

To verify the accuracy of the present findings, a 3-D FE simulation is also carried out in COMSOL Multiphysics commercial software COMSOL, 2016. To this end, a flexible micro-plate with fully clamped boundary conditions has been modeled using 3-D brick elements together with the physics of *Electromechanics*. It is to be mentioned here that this physics combines the physics of solid mechanics and electrostatics with a moving mesh to simply model the deformation of electrically actuated structures. Stationary and time-dependent studies have also been selected to provide static and dynamic results, respectively.

For the purpose of validation, a square silicon micro-plate with $\alpha_3 = 1$ and other properties presented in Table 3 is considered. Figure 2 verifies

Table 3. Geometric and material properties of a square silicon micro-plate (Osterberg, 1995).

$a(\mu m)$	$h(\mu m)$	E(GPa)	ν	$\rho(kg/m^3)$
1000	3	169	0.3	2332

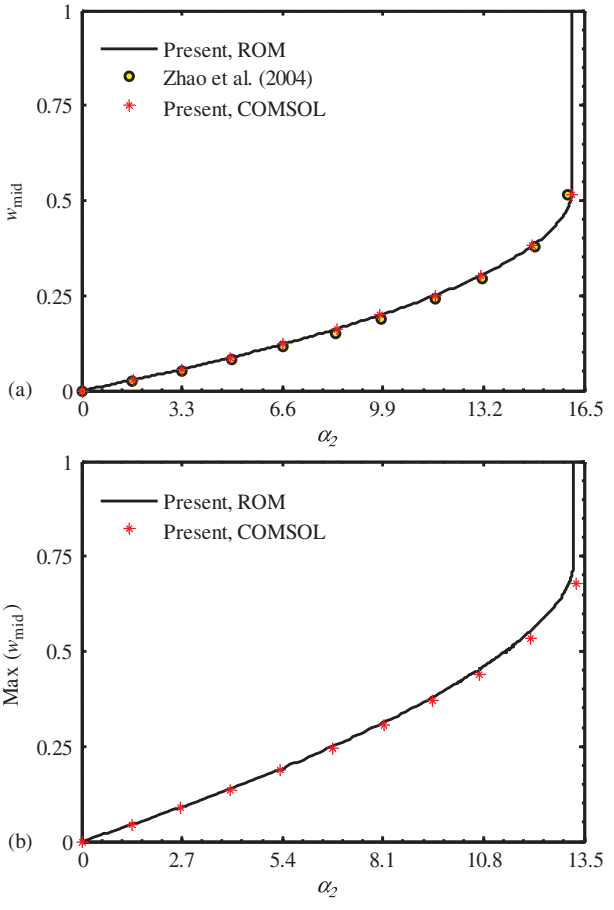

Figure 2. Verification of the (a) static and (b) dynamic responses of a micro-plate with normalized properties $\alpha_3 = 1$ and $\nu = 0.3$ over its whole operation range.

the accuracy of both static and dynamic responses of the present micro-plate over its whole operation range. Figure 2(a) compares the static values of the micro-plate mid-point deflection by those reported in the literature (Zhao et al., 2004) as well as the ones obtained via 3-D FE simulations in COMSOL (Version 5.2a, 2016). Also, Figure 2(b) provides a comparison between the maximum dynamic values of the micro-plate mid-point deflection and those achieved through 3-D FE simulations.

According to the results shown in Figure 2, the present RO and FE findings in both static and dynamic cases are in excellent agreement with each other. Also, all of the present static findings, which are obtained by the RO procedure and 3-D FE simulations, match with those reported by Zhao et al. (2004) very well.

Table 4 provides verifications for the converged static and dynamic pull-in parameters of micro-plates with properties given in Table 3 and different initial gaps. Besides a comparison between the present RO and 3-D FE results, this table compares all the present findings by those available in the literature for statically excited systems (Batra et al., 2008b; Zhao et al., 2004). According to Table 4, the present RO and FE findings are in full agreement with each other in both static and dynamic loading cases. Furthermore, the present static predictions especially for systems with large initial gaps, which suffer from strong non-linearities (Zhao et al., 2004), agree with the FE results better than those reported by Zhao et al. (2004). Hence, using the present ROM is strongly suggested for both static and dynamic pull-in analysis of plate-type MEMS; because it not only does not suffer from the long run-time but also is so accurate and reliable in comparison to 3-D FE simulations.

As it is mentioned earlier, the main object of the present paper is to answer the basilar question of how many natural modes for discretising the in- and out-of-plane displacements should be included to ensure an efficient ROM. In view of the results reported in Tables 1 and 2, one can answer this question as: *employing only one out-of-plane natural mode is sufficient for the convergence of the results; however, each in-plane displacement needs to be approximated using at least four basis functions* (i.e. $n = 2$). This is due to the fact that the deformed configuration of the transverse deflection is very similar to the first natural mode of the micro-plate, but the final shape of each in-plane

Table 4. Verification of the static and dynamic pull-in parameters for a square micro-plate with different gaps and $\nu = 0.3$.

Analysis	Method	$\alpha_3 = 1$	$\alpha_3 = 1.5$	$\alpha_3 = 2$
Static	Present	16.06	18.73	22.97
	COMSOL	16.06	18.75	23.05
	Zhao et al. (2004)	16.00	18.48	22.43
	Batra et al. (2008b)	16.33	–	–
Dynamic	Present	13.26	15.27	18.35
	COMSOL	13.30	15.31	18.40

displacement includes at least the first four natural modes of the system (Batra et al., 2008b). Therefore, one can conclude that the previous studies which neglected the effect of in-plane displacements (Nabian et al., 2013; Talebian et al., 2010) or approximated each of them using less than four natural modes (i.e. $n < 2$) (Mohammadi & Ali, 2015) may not be accurate. It is to be mentioned here that, in view of Tables 1 and 2, although employing 18 in-plane natural modes (i.e. $n = 3$) is essential for full convergence, the results will be accurate enough if eight in-plane natural modes (i.e. $n = 2$) are utilised.

To investigate the influence of in-plane displacements on the accuracy of the results, Figure 3 illustrates the convergence of both in- and out-of-plane time histories for a square micro-plate with $\alpha_3 = 1$ and other properties given

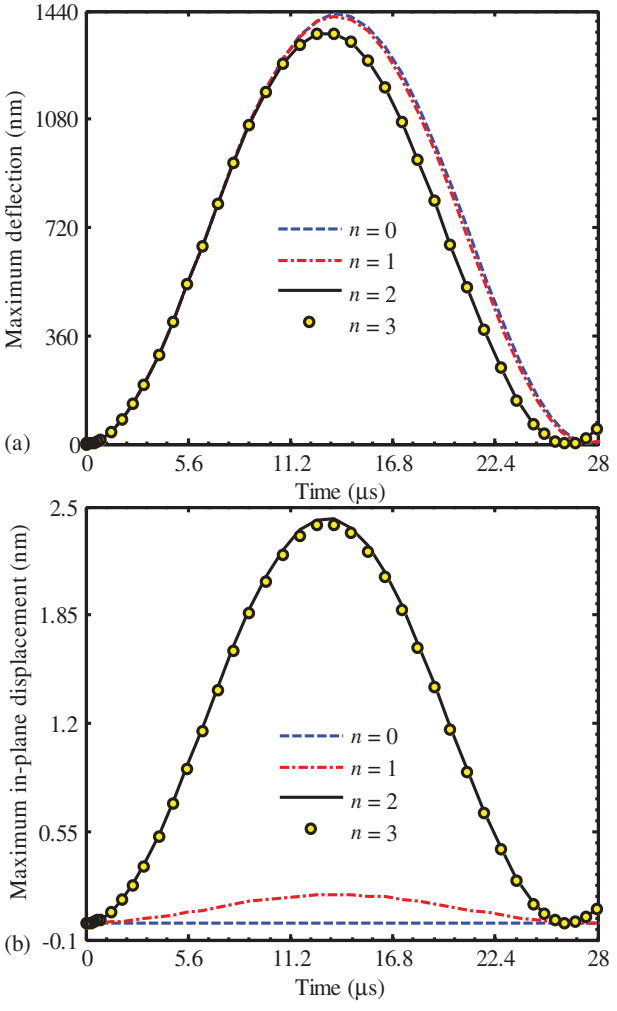

Figure 3. Time histories of the maximum in- and out-of-plane displacements for a square micro-plate with $\alpha_3 = 1$ and other properties presented in Table 3 under an input voltage of $V_{DC} = 0.9V_{DPI}$.

in Table 3. It is assumed that the input voltage equals to 90% of the micro-plate dynamic pull-in counterpart and the maximum values of the in- and out-of-plane time histories are selected just for the sake of improving the quality of presentation. It is worth mentioning that the maximum time histories occur at $\hat{x} = 0.16a,\ \ \hat{y} = 0$ for the in-plane displacement u, $\hat{x} = 0,\ \ \hat{y} = 0.16b$ for the in-plane displacement v and $\hat{x} = 0,\ \hat{y} = 0$ for the out-of-plane displacement w. In addition, since the present micro-plate takes the square shape, the time histories of the maximum in-plane displacements are the same. Hence, just for the sake of brevity, only one of the in-plane time histories is depicted in Figure 3.

As Figure 3 illustrates, it is apparent that both in- and out-of-plane vibration frequencies of the micro-plate as well as its amplitudes are converged when at least eight in-plane basis functions (i.e. $n = 2$) are employed. In addition, according to this figure, it is obvious that although in-plane displacements take so negligible values in comparison to the micro-plate transverse deflection, ignoring these parts of the displacement field results in producing inaccurate out-of-plane findings. Therefore, one can say that accounting for the influences of the in-plane displacements is so essential in pull-in analysis; because they seriously affect the accuracy of the out-of-plane findings and all quantities related to it such as the micro-plate instability thresholds.

Figure 4 provides the final configurations of the maximum displacements for the previous case study occurring at $\hat{t} = 13.4\,\mu$s. According to this figure, the final configuration of the micro-plate transverse deflection is very similar to the clamped plates' first natural mode. That is the reason for the fact that the out-of-plane displacement needs to be approximated only using one natural mode. However, according to Figure 4, the final configurations of the in-plane displacements require more than one natural mode for the convergence.

It is to be noted that the convergence speed of the results seriously depends on the particular shapes of the basis functions. Therefore, different ROMs with different approximating functions may require different numbers of basis functions to be convergent. In this way, consider the work done by Saghir and Younis (2016). They approximated the in-plane displacements of the system using only one basis function which was extracted from the FE simulation of a micro-plate under uniform pressure in COMSOL Multiphysics commercial software (Saghir & Younis, 2016). Figure 5 represents a comparison between the present RO findings and those of Saghir and Younis (2016) for a micro-plate with properties presented in Table 5.

According to Figure 5, the present findings agree excellently with those reported by Saghir and Younis (2016). That is due to the fact that the deformed shapes of the in-plane displacements under electrical loading are very similar to the basis functions employed by Saghir and Younis (2016). Hence, it can be concluded that if the selected basis functions are similar to the deformed shape

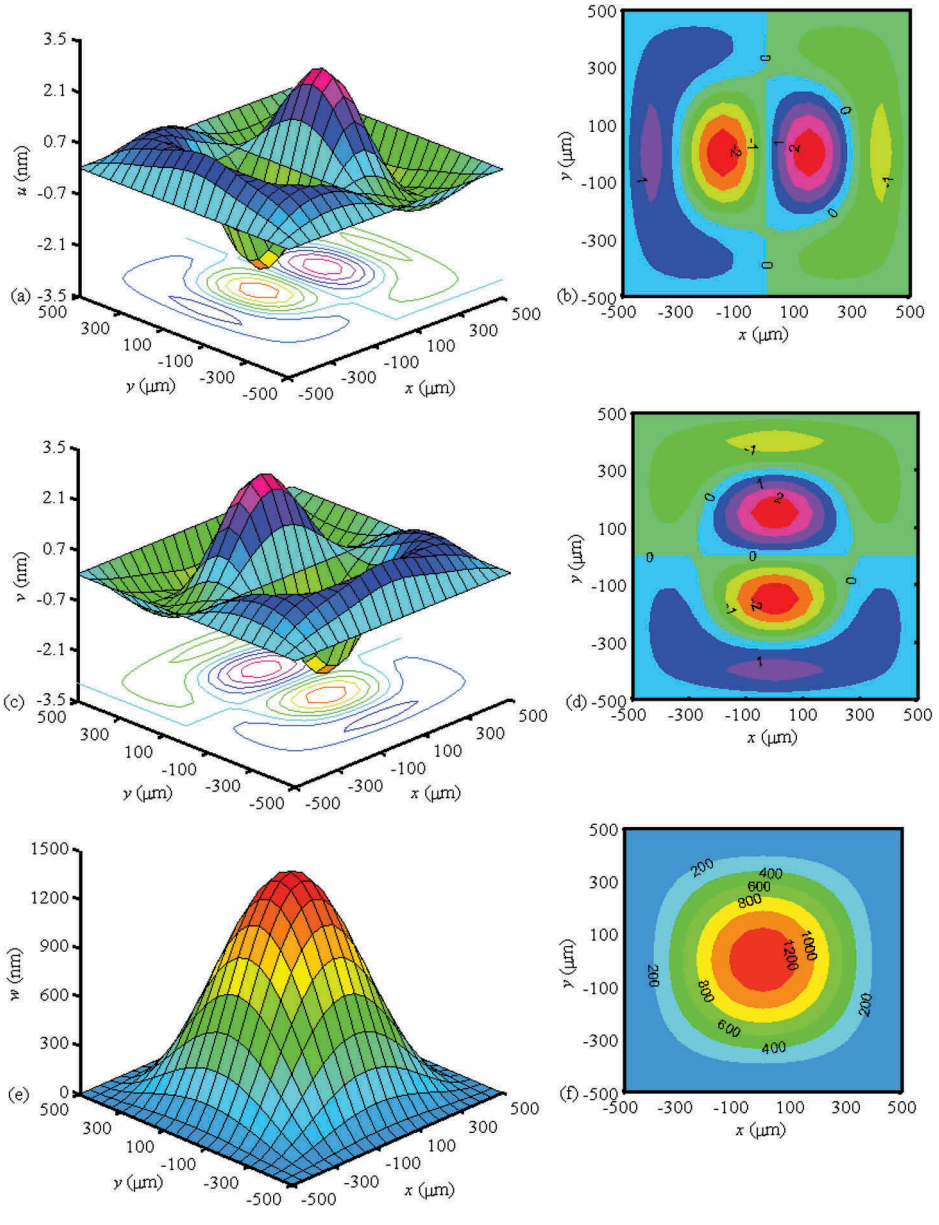

Figure 4. The maximum in- and out-of-plane displacements (a, c, e) and their corresponding contour plots (b, d, f) for a square micro-plate with $a_3 = 1$ and other properties presented in Table 3 under an input voltage of $V_{DC} = 0.9V_{DPI}$.

of a displacement, the solution will be converged through employing only one basis function for approximating the respective displacement.

As it was mentioned above, employing only the first natural mode in the transverse direction is sufficient for converging the results; however, some previous studies (Saghir & Younis, 2016; Zhao et al., 2004) believed that it is so necessary to account for the effect of higher out-of-plane natural

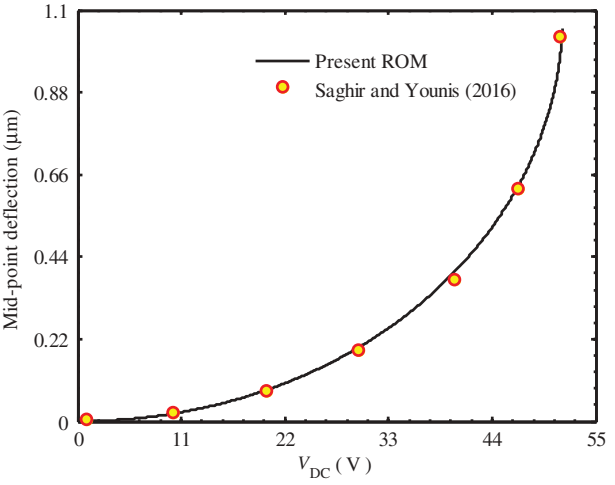

Figure 5. Comparison between the present findings and those reported by Saghir and Younis (2016) for a micro-plate with properties presented in Table 5.

Table 5. Geometric and material properties of a micro-plate investigated by Saghir and Younis (2016).

$a(\mu m)$	$b(\mu m)$	$h(\mu m)$	$d(\mu m)$	E(GPa)	ν
300	450	2	2	153	0.23

modes. This contrast between the present conclusion and that reported by Zhao et al. (2004) as well as Saghir and Younis (2016) is due to the fact that the authors of these papers pre-multiplied the transverse governing equation of motion by the denominator of the electrostatic forcing term which results in changing the weighting functions of the GWRM (Gutschmidt, 2010) and so in its convergence speed. Therefore, they were forced to employ higher transverse natural modes for generating a convergent ROM with accurate results.

4.2. *Effect of micro-structure inertia*

According to the results presented in Table 4 and Figure 2, it is obvious that accounting for the influence of micro-structure inertia reduces the instability threshold of the system. To investigate this issue more, Figure 6 depicts the variation of the dynamic to static pull-in voltages ratio, which is calculated as $\sqrt{\alpha_2^{\mathrm{DPI}}/\alpha_2^{\mathrm{SPI}}}$, versus the aspect ratio of the system at some different gap parameters. As Figure 6 illustrates, dynamic pull-in voltages in plate-type MEMS usually take values around 90% of the static counterparts. It is worth noting that this ratio for doubly clamped micro-beams was reported as $V_{\mathrm{DPI}}/V_{\mathrm{SPI}} \approx 91 - 92\%$ (Chao, Chiu, & Liu, 2008). Hence, it can be concluded

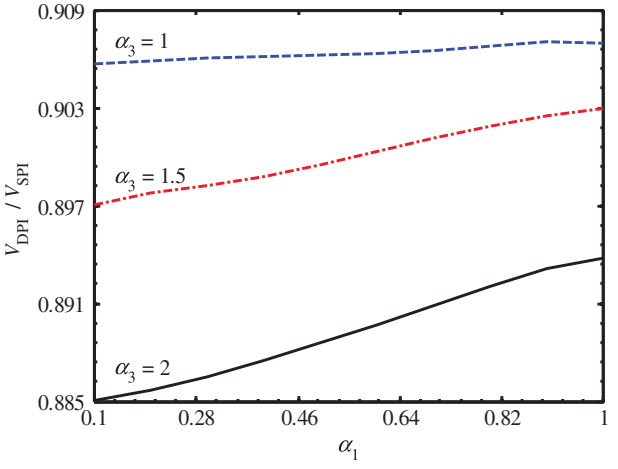

Figure 6. Effect of inertia on the instability threshold of systems with different gap parameters and aspect ratios.

that the micro-structure inertia plays a more crucial role in reducing the instability threshold of plate-type MEMS than that of beam-type ones.

In view of the results presented in Figure 6, one can observe that the ratio of dynamic to static pull-in voltages reduces with an increase of the gap parameter. This fact means that increasing the gap between the two electrodes increases the effect of micro-structure inertia. Therefore, it is more important to account for the effect of inertia in the calculation of pull-in voltage for MEMS devices with larger initial gaps. Furthermore, based on the results of Figure 6, it is seen that increasing the aspect ratio of the micro-plate increases the ratio of dynamic to static pull-in voltages. Hence, one can conclude that the effect of micro-structure inertia is the minimum for micro-plates with the square shape.

Figure 7 represents the variation of the geometric non-linear to linear pull-in voltages ratios versus the micro-plate aspect ratio in both static and dynamic loading cases. As this figure depicts, accounting for the effect of micro-structure inertia slightly reduces the influence of geometric non-linearity. In addition, based on the results shown in this figure, increasing the values of the gap parameter increases the influence of inertia on reducing the geometric non-linearity effect. Furthermore, one can observe that increasing the micro-plate aspect ratio decreases the effect of geometric non-linearity in both static and dynamic cases. Therefore, the influence of the geometric non-linearity is the minimum for square micro-plates in both static and dynamic loading cases. It is to be mentioned here that a similar conclusion for statically excited rectangular micro-plates has also been reported by Batra et al. (2008b).

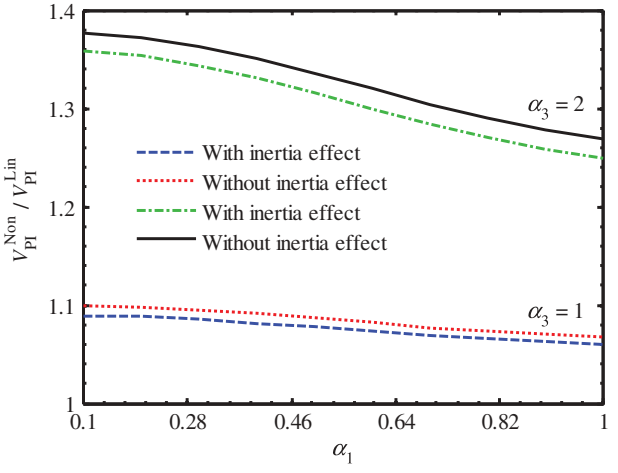

Figure 7. Effect of geometric non-linearity on the instability threshold of the system in both static and dynamic loading cases.

5. Concluding remarks

The present paper aimed to answer the important question of how many natural modes have to be considered in generating a ROM for plate-type MEMS to ensure its convergence. For this object, a full geometric non-linear Kirchhoff's plate model, which includes the effect of in-plane displacements, was considered. The system of governing equations of motion was solved by a multi-term ROM in which the transverse approximating functions had been obtained by the extended Kantorovich method. The minimum numbers of in- and out-of-plane natural modes were obtained by performing a convergence study on the values of both dimensionless static and dynamic pull-in voltages of the system. The results revealed that the transverse deflection of the micro-plate can be approximated using only its first natural mode. However, at least four eigen modes for each in-plane displacement should be included into the ROM to give a converged solution. The results of the present fast convergent ROM were also verified by those simulated using COMSOL Multiphysics commercial FE package as well as the available static findings in the literature. It was found that the present static predictions agreed with those obtained by 3-D FE simulations better than the available results in the previous studies. At the rest of the paper, the present so rapid ROM was employed to investigate the influence of micro-structure inertia on the instability threshold of the system. The main conclusions which can be drawn from this section of the present study can be summarised to:

- The instability threshold of electrically actuated fully clamped rectangular micro-plates is affected by the micro-structure inertia more than that of doubly clamped beam-type MEMS.

- In general, accounting for the influence of micro-structure inertia decreases the instability threshold of the system. That is the dynamic pull-in voltage in plate-type MEMS usually takes a value around 90% of its static counterpart.
- The effect of micro-structure inertia, which is the minimum for micro-plates with square shapes, increases with an increase of the gap parameter.
- The influence of the geometric non-linearity in dynamically excited systems is lower than those actuated statically. Furthermore, this effect is the minimum for micro-plates with square shapes.

Disclosure statement

No potential conflict of interest was reported by the author.

ORCID

Amir R Askari http://orcid.org/0000-0002-8090-7926

References

Amabili, M. (2004). Nonlinear vibrations of rectangular plates with different boundary conditions: theory and experiments. *Computers & Structures*, *82*(31–32), 2587–2605.

Ansari, R., Gholami, R., Mohammadi, V., & Faghih Shojaei, M. (2012). Size-dependent pull-in instability of hydrostatically and electrostatically actuated circular microplates. *Journal of Computational and Nonlinear Dynamics*, *8*(2), 021015.

Batra, R. C., Porfiri, M., & Spinello, D. (2007). Review of modeling electrostatically actuated microelectromechanical systems. *Smart Materials and Structures*, *16*, 23–31.

Batra, R. C., Porfiri, M., & Spinello, D. (2008a). Effects of van der Waals force and thermal stresses on pull-in instability of clamped rectangular microplates. *Sensors*, *8*(2), 1048–1069.

Batra, R. C., Porfiri, M., & Spinello, D. (2008b). Reduced-order models for microelectromechanical rectangular and circular plates incorporating the Casimir force. *International Journal of Solids and Structures*, *45*, 3558–3583.

Chao, P. C. P., Chiu, C. W., & Liu, T. H. (2008). DC dynamic pull-In predictions for a generalized clamped–clamped microbeam based on a continuous model and bifurcation analysis. *Journal of Micromechanics and Microengineering*, *18*(p), 115008.

Chao, P. C. P., Chiu, C. W., & Tsai, C. Y. (2006). A novel method to predict the pull-in voltage in a closed form for micro-plates actuated by a distributed electrostatic force. *Journal of Micromechanics and Microengineering*, *16*, 986–998.

COMSOL Multiphysics, Version 5.2a, Burlington, MA 01803 (http://www.comsol.com). (2016).

Faires, J. D., & Burden, R. L. (2002). *Numerical methods* (3rd ed.). CA: Brooks/Cole.

Gutschmidt, S. (2010). The influence of higher-order mode shapes for reduced-order models of electrostatically actuated microbeams. *Journal of Applied Mechanics*, *77*(4), 041007–410076. doi:10.1115/1.4000911

Jones, R., & Milne, B. J. (1976). Application of the extended Kantorovich method to the vibration of clamped rectangular plates. *Journal of Sound and Vibration*, *45*(3), 309–316.

Mohammadi, A. K., & Ali, N. A. (2015). Effect of high electrostatic actuation on thermo-elastic damping in thin rectangular microplate resonators. *Journal of Theoretical and Applied Mechanics*, *53*(2), 317–329.

Nabian, A., Rezazadeh, G., Almassi, M., & Borgheei, A.-M. (2013). On the stability of a functionally graded rectangular micro-plate subjected to hydrostatic and nonlinear electrostatic pressures. *Acta Mechanica Solida Sinica*, *26*(2), 205–220.

Osterberg, P. M. (1995). *Electrostatically Actuated Microelectromechanical Test Structures for Material Property Measurement* PhD Dissertation. Massachusetts Institute of Technology.

Saghir, S., & Younis, M. I. (2016). An investigation of the static and dynamic behavior of electrically actuated rectangular microplates. *international Journal of Non-Linear Mechanics*, *85*, 81–93.

Senturia, S. D. (2001). *Microsystem Design*. Dordrecht: Kluwer Academic Publishers.

Tajalli, S. A., Moghimi Zand, M., & Ahmadian, M. T. (2009). Effect of geometric non-linearity on dynamic pull-in behavior of coupled-domain microstructures based on classical and shear deformation plate theories. *European Journal of Mechanics – A/Solids*, *28*(5), 916–925.

Talebian, S., Rezazadeh, G., Fathalilou, M., & Toosi, B. (2010). Effect of temperature on pull-in voltage and natural frequency of an electrostatically actuated microplate. *Mechatronics*, *20*(6), 666–673.

Wang, B., Zhou, S., Zhao, J., & Chen, X. (2011). Pull-in instability analysis of electro-statically actuated microplate with rectangular shape. *International Journal of Precision Engineering and Manufacturing*, *12*(6), 1085–1094.

Younis, M. I. (2011). *MEMS linear and nonlinear statics and dynamics*. New York: Springer.

Zhao, X., Abdel-Rahman, E. M., & Nayfeh, A. H. (2004). A reduced-order model for electrically actuated microplates. *Journal of Micromechanics and Microengineering*, *14*, 900–906.